Time-dependent configuration-interaction calculations of laser-driven dynamics in presence of dissipation

Jean Christophe Tremblay, Tillmann Klamroth, and Peter Saalfrank

Citation: J. Chem. Phys. **129**, 084302 (2008); doi: 10.1063/1.2972126
View online: http://dx.doi.org/10.1063/1.2972126
View Table of Contents: http://jcp.aip.org/resource/1/JCPSA6/v129/i8
Published by the American Institute of Physics.

Time-dependent configuration-interaction calculations of laser-driven dynamics in presence of dissipation

Jean Christophe Tremblay,[a] Tillmann Klamroth, and Peter Saalfrank[b]
Institut für Chemie, Universität Potsdam, Karl-Liebknecht-Straße 24-25, D-14476 Potsdam-Golm, Germany

(Received 9 July 2008; accepted 29 July 2008; published online 22 August 2008)

Correlated, multielectron dynamics of "open" electronic systems within the fixed-nuclei approximation are treated here within explicitly time-dependent configuration-interaction schemes. Specifically, we present simulations of laser-pulse driven excitations of selected electronic states of LiCN in the presence of energy and phase relaxation. The evolution of the system is studied using open-system density matrix theory, which embeds naturally in the time-dependent configuration-interaction singles (doubles) formalism. Different models for dissipation based on the Lindblad semigroup formalism are presented. These models give rise to lifetimes for energy relaxation ranging from a few hundreds of femtoseconds to several nanoseconds. Pure dephasing is treated using a Kossakowski-like Gaussian model, proceeding on similar time scales. The pulse lengths employed range from very short (tens of femtoseconds) to very long (several nanoseconds). To make long-time propagations tractable, the quasiresonant approximation is used. The results show that despite the loss of efficiency, selective dipole switching can still be achieved in the presence of dissipation when using appropriately designed laser pulses. © *2008 American Institute of Physics*. [DOI: 10.1063/1.2972126]

I. INTRODUCTION

Nowadays the electronic structure of small isolated molecules can be routinely characterized using a variety of very efficient methods, ranging from *ab initio* schemes[1] to density functional theory (DFT).[2,3] In particular, time-dependent variants of DFT methods (TD-DFT) are very useful in studying excited electronic states and their associated properties.[4,5] Typically, TD-DFT is mostly formulated in the frequency domain and in the linear response regime. Explicitly time-dependent variants of DFT have also been used but still have some limitations: It is difficult to improve TD-DFT systematically toward the exact solution of the time-dependent electronic Schrödinger equation. It is thus not easy to treat long-range charge transfer, Rydberg states, van-der Waals forces, and static correlation. Further, being a method based on the Schrödinger equation, it is also not made for "open systems," i.e., quantum systems coupled to a bath, which accounts for energy and phase relaxation. The latter, however, are important if one wishes to treat, for example, quantum transport through molecular junctions.

Recently, Di Ventra and D'Agosta[6] proposed a time-dependent current DFT approach to extend the applicability of DFT methods to open systems. The dynamical interaction of the subsystem and the environment has been included by means of a stochastic perturbation to the equation of motion of a single Kohn–Sham Slater determinant. It was shown that at least in some cases, the convergence of the stochastic process is very fast and that dissipation can be treated efficiently.[6,7] As an example, the spontaneous emission in atoms after laser excitation was treated.[7]

Time-dependent *ab initio* methods, such as TD-Hartree–Fock,[8] TD-configuration interaction,[9] and TD-CASSCF (Refs. 10–12) represent alternatives to TD-DFT. The multideterminant variants time-dependent configuration interaction (TD-CI) and time-dependent complete active space self-consistent field (TD-CASSCF) can yield accurate energies for the ground state as well as for many excited electronic states. Apart from being systematically improvable, TD-CI and TD-CASSCF methods provide also the right asymptotics to treat long-range problems of the type described above. Thus, the TD-CI method has been successfully applied to photoemission from metal films,[13,14] laser-induced intra-[15,16] and intermolecular charge transfer,[17] laser-induced electron transfer through metal-insulator-metal junctions,[9,18] the creation of electronic wavepackets,[15,19] and the calculation of response properties of molecules following time-dependent perturbations.[19] In the TD-CI methods the electronic wave function is expanded using a set of predetermined electronic eigenstates Ψ_i with energies E_i as $\Psi = \Sigma_i C_i(t)\Psi_i$, where only the expansion coefficients C_i depend on time. These *ab initio* methods provide a very natural and attractive way to study open-system dynamics: One simply represents the subsystem evolutions using the reduced density matrix formalism in the basis of these eigenstates. The effect of the environment is taken into account as a dissipative term in the equations of motion of the subsystem. Here we make the Markov approximation and assume the Lindblad semigroup form for this dissipative contribution.

We propose here to study the effect of different dissipa-

[a]Electronic mail: jean.c.tremblay@gmail.com.
[b]Electronic mail: petsaal@rz.uni-potsdam.de.

tive mechanisms on the dynamics of a simple molecule. Namely, we will perform laser excitations of selected electronic states of LiCN, which serves as a model system for exploring dipole switching processes. The molecule has been studied before by Krause *et al.*[15] using TD-CI methods, without considering environmental effects. It was shown that dipole switching could be achieved selectively for reasonably short pulses with appropriate polarization. To treat the coupling of the molecule to a "bath," the semigroup formalism is used to introduce the effect of pure dephasing and energy relaxation within the system.[20–25] It will be shown that the dynamics of the system is indeed affected by dissipation but that selectivity can be maintained to some extent.

This paper is organized as follows. In Sec. II we recall the time-dependent configuration-interaction singlets (doublets) [CIS(D)] method and briefly discuss the properties of the system. The propagation schemes will then be introduced as well as the three dissipation models to be studied. In Sec. III we perform selective excitations of charge transfer states and analyze the behavior of the system subject to the different dissipation models introduced in Sec. II. The most important results are then summarized in Sec. IV.

II. THEORY

A. Configuration-interaction calculations

The field-free electronic Hamiltonian representing an N electrons, N_A nuclei molecule is given, in atomic units ($\hbar = 4\pi\epsilon_0 = m_e = e = 1$), by

$$\hat{H}_0 = -\frac{1}{2}\sum_{i=1}^{N}\Delta_i + \sum_{i=1}^{N}\sum_{j<i}^{N}\frac{1}{r_{ij}} - \sum_{i=1}^{N}\sum_{k=1}^{N_A}\frac{Z_A}{r_{Ai}}, \tag{1}$$

where $-\frac{1}{2}\Delta_i$ is the single-electron kinetic energy operator, r_{ij} is the distance between electrons i and j, r_{Ai} is the distance between electrons i and nucleus A, and Z_A is the charge of the Ath nucleus. In the CIS(D) formalism advocated here, one first computes spatial molecular orbitals at the restricted Hartree–Fock level using the ground state Slater determinant (Ψ^{HF}) as a trial wave function. Exciting one electron from occupied orbital a to unoccupied orbital r allows generating a set of excited configurations (Ψ_a^r), which are then used as a basis to represent the full Hamiltonian, Eq. (1). The resulting matrix can be diagonalized to yield the CIS eigenvalues E_i^{CIS} and eigenfunctions Ψ_i. The ith wave function Ψ_i has the general form

$$\Psi_i = D_{0,i}\Psi_0^{HF} + \sum_{a=L}^{N/2}\sum_{r=N/2+1}^{M} D_{a,i}^r\, {}^1\Psi_{a,r}, \tag{2}$$

where D are expansion coefficients, L is the index of the lowest occupied orbital, and M is the index of the highest unoccupied orbital. In Eq. (2) and in the following, only singlet configuration state functions ${}^1\Psi_a^r = 1/\sqrt{2}(\Psi_a^r + \Psi_{\bar{a}}^{\bar{r}})$ (with a, r referring to α and $\bar{a}$, $\bar{r}$ referring to β spin orbitals) were used to construct singlet wave functions Ψ_i because only those are optically accessible from a singlet Hartree–Fock ground state Ψ_0^{HF}, which is always employed as the initial state below. In the CIS(D) method, the eigenvalues are further corrected by perturbation theory to account for double excitations, i.e., $E_i^{\mathrm{CIS(D)}} = E_i^{\mathrm{CIS}} + E_i^{(\mathrm{D})}$. Here, $E_i^{(\mathrm{D})}$ are correction terms that are defined elsewhere.[26] In CIS(D), also the ground state energy is correlation corrected giving the same energy as Møller–Plesset perturbation theory to second order (MP2).

B. Laser excitation of the LiCN molecule

In the present work we perform laser-induced dipole switching calculations of singlet states of a linear LiCN molecule in its HF/6–31G* equilibrium geometry ($R_{\mathrm{Li-C}} = 3.683\ a_0$, $R_{\mathrm{C-N}} = 2.186\ a_0$). Using a 6–31G* atomic orbital basis and the GAMESS program[27] to obtain the molecular orbitals, we find 186 singlet CIS(D) states up to about $5E_h$ above the ground state.[28] In particular we will be interested in the switching between states $|0\rangle$, $|2\rangle$, and $|9\rangle$. States $|2\rangle$ and $|3\rangle$ are degenerate and state $|9\rangle$ is degenerate with state $|8\rangle$. With the molecule oriented along the z-axis, these states have permanent dipole moments of −3.7082, +2.7952, and −1.1777 ea_0, respectively, the energy differences are $\Delta E_{02} = 0.2254$ and $\Delta E_{29} = 0.2747E_h$ ($1\ E_h$="Hartree" $= 27.211$ eV), respectively. Thus when switching from $|0\rangle$ to $|2\rangle$ the dipole moment is reversed. This is due to an intramolecular charge transfer, dominated by a $\pi \rightarrow \sigma^*$ transition, which effectively transfers an electron from CN to Li.[15] The transition is dominantly x-polarized, with a transition dipole $\mu_{0,2;x} = +0.3084ea_0$. (A small y-component is neglected here, see Table I of Ref. 15.) The semicovalent state $|9\rangle$ is readily accessible from there also with x-polarized light, $\mu_{2,9;x} = -1.0333ea_0$. In this case about half an electron is transferred from Li back to CN, as detailed elsewhere.[15]

The transition from the ground state $|0\rangle$ or the intermediate state $|2\rangle$ to the target levels $|2\rangle$ or $|9\rangle$, respectively, can be achieved by x-polarized π-pulse excitations. Treating the interaction of the molecule and a laser field $E_x(t)$ in the semiclassical dipole approximation, the total Hamiltonian of the dissipation-free system has the form

$$\hat{H} = \hat{H}_0 - \hat{\mu}_x E_x(t). \tag{3}$$

Here, $\hat{\mu}_x$ is the x-component of the total dipole operator $\hat{\underline{\mu}} = -\Sigma_i^N \underline{r}_i + \Sigma_{A=1}^{N_A} Z_A \underline{R}_A$. In Eq. (3), the n-component field is given by

$$E_x(t) = \sum_{k=1}^{n} E_k(t)\cos(\omega_k t),$$
$$E_k(t) = \begin{cases} E_{0,k}\sin^2\left(\dfrac{\pi(t-t_{k_1})}{2(t_{k_2}-t_{i_1})}\right) & \text{if } t_{k_1} \le t \le t_{k_2} \\ 0 \quad \text{otherwise.} \end{cases} \tag{4}$$

t_{k_1} (t_{k_2}) is the kth pulse starting (finishing) time. The individual π-pulses, which cause population inversion in an ideal, dissipation-free two-level system under the rotating wave approximation, have fluences given by $F_k = (3\pi c/16) \times [1/(t_{i_2} - t_{i_1})|\mu_{fi}|^2]$, where c is the velocity of light and μ_{fi} is the x-component of the transition dipole moment, $\langle f|\hat{\mu}_x|i\rangle$, which connects the initial ($|i\rangle = |0\rangle$ or $|2\rangle$) and final ($|f\rangle = |2\rangle$ or $|9\rangle$) states.

In Ref. 15, all states Ψ_i obtained from CIS(D) were treated as stationary and laser-induced transitions between them were modeled by solving the time-dependent Schrödinger equation

$$i\frac{\partial\Psi(t)}{\partial t} = \hat{H}(t)\Psi(t) \tag{5}$$

in the basis of the CIS(D) eigenstates. In the present work, we use an open-system density matrix description instead to treat energy and phase relaxation.

C. Treatment of dissipation

In order to characterize the dynamics of the system in presence of dissipation we advocate using the reduced density matrix formalism.[29] The evolution of the density operator, $\hat{\rho}(t)$, obeys the Liouville–von Neumann equation

$$\frac{\partial\hat{\rho}(t)}{\partial t} = -i[\hat{H},\hat{\rho}(t)] + \mathcal{L}_D\hat{\rho}(t). \tag{6}$$

The precise form of the dissipative Liouvillian, $\mathcal{L}_D$, depends on the model used for representing dissipation.

The semigroup formalism is very appealing in studying factors affecting the quantum dynamics of open systems. It was pioneered by Gorini and co-workers.[20,21] We will stick to the formalism developed by Lindblad.[22] It has the advantage of ensuring semipositivity of the reduced density matrix. This allows interpretation of its diagonal elements, in the CIS(D) approximate eigenstate basis, as population of these zeroth order states. The Lindblad dissipative Liouvillian has the general form

$$\mathcal{L}_D\hat{\rho} = -\frac{1}{2}\sum_k \{[\hat{C}_k\hat{\rho},\hat{C}_k^\dagger] + [\hat{C}_k,\hat{\rho}\hat{C}_k^\dagger]\}, \tag{7}$$

where $\hat{C}_k$ is a Lindblad operator, appropriately chosen to represent a dissipation channel k.

In what follows we study the effect of energy relaxation in LiCN using raising/lowering operators as Lindblad operators,[23] i.e.,

$$\hat{C}_k \to \sqrt{\Gamma_{m\to n}}|n\rangle\langle m|, \tag{8}$$

where $|n\rangle = \Psi_n$ is one of the L electronic states and $\Gamma_{m\to n}$ is the bath-induced transition rate between states $|m\rangle$ and $|n\rangle$. In the basis of the subsystem eigenstates the time evolution of the matrix elements of the density operator then becomes

$$\frac{d\rho_{nn}}{dt} = -iE_x(t)\sum_{i=1}^{L}(\mu_{ni}\rho_{in} - \rho_{ni}\mu_{in}) + \sum_{i=1}^{L}(\Gamma_{i\to n}\rho_{ii} - \Gamma_{n\to i}\rho_{nn}), \tag{9}$$

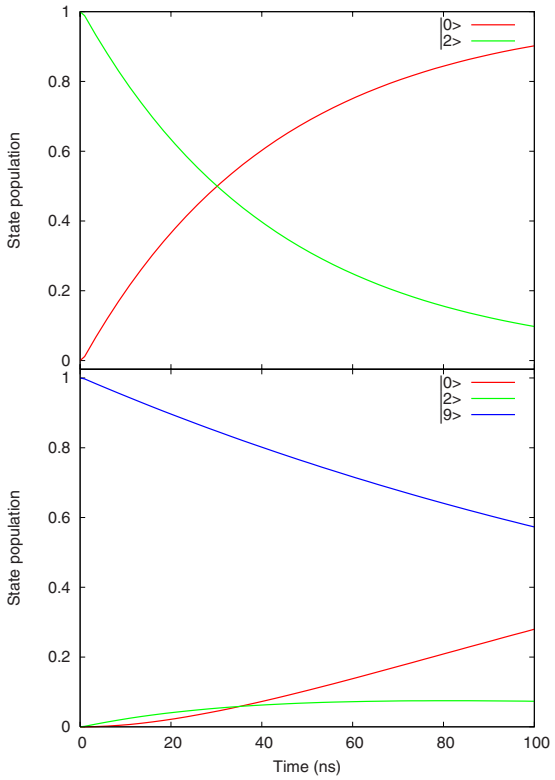

FIG. 1. (Color online) Free decay of state $|2\rangle$ (top panel) and $|9\rangle$ (lower panel) at 0 K for the radiative lifetime (spontaneous emission) model. The transition $|2\rangle\to|0\rangle$ has a lifetime of about 43 ns and the transition $|9\rangle\to|2\rangle$ has a lifetime of about 360 ns.

$$\frac{d\rho_{mn}}{dt} = -i\omega_{mn}\rho_{mn} - iE_x(t)\sum_{i=1}^{L}(\mu_{mi}\rho_{in} - \rho_{mi}\mu_{in}) - \gamma_{mn}\rho_{mn}. \tag{10}$$

Here, $\omega_{mn} = E_m^{\mathrm{CIS(D)}} - E_n^{\mathrm{CIS(D)}}$. At zero temperature only downward transitions are possible, which is the case here. Furthermore, $\gamma_{mn} = \gamma_{nm} = 1/2\Sigma_l^L(\Gamma_{m\to l} + \Gamma_{n\to l})$ is the dephasing rate in which pure dephasing is not yet included.

To evaluate the downward transition rates, we choose to use the Einstein coefficient A_{mn} for spontaneous emission from a higher state $|m\rangle$ to a lower state $|n\rangle$, thus treating the case of coupling through the vacuum. The coefficients read

$$\Gamma_{m\to n} = \frac{4n|\mu_{mn}^{\mathrm{tot}}|^2}{3c^3}\omega_{mn}^3, \tag{11}$$

where $\mu_{mn}^{\mathrm{tot}} = (\mu_{mn,x}^2 + \mu_{mn,y}^2 + \mu_{mn,z}^2)^{1/2}$ is the total transition dipole moment, and n is the refractive index ($n=1$ in vacuum). We note in passing that coefficients depend cubically on the energy difference between two levels, ω_{nm}. These transition rates give rise to lifetimes greater than about 10 ns for the states of interest. Figure 1 shows the free decay of states $|2\rangle$ and $|9\rangle$ calculated using this model. The decay of state $|2\rangle$ can be seen from the top panel, where only the transition to the ground state is significant. The corresponding radiative lifetime is $\tau_{\mathrm{rad}} = \Gamma_{2\to 0}^{-1} = 43$ ns. At the bottom panel we see that the decay of state $|9\rangle$ goes first through state $|2\rangle$, followed by relaxation to the ground state. This state decays

within 360 ns. The first excited state, $|1\rangle$, is z-polarized and has a radiative lifetime of 26 ns.

To simulate the interaction of the molecule with an environment favoring energy relaxation, such as a metal surface, we simply scale the radiative transition rate by an arbitrary factor (ϵ), i.e., $\tilde{\Gamma}_{m\to n}=\epsilon\cdot\Gamma_{m\to n}$. We choose to set $\epsilon=10^5$. We dub this somewhat arbitrary model the *surface enhanced relaxation approach* (SERA). The SERA lifetimes are, accordingly, by this factor shorter than the spontaneous emission lifetimes of an isolated molecule, i.e., about 430 fs for the $|2\rangle$ state. Note that this value is still not unrealistically short, at least not for electronically excited molecules at metal surfaces, for which lifetimes of a few femtoseconds are the rule rather than the exception.[30]

We can also study the effect of pure dephasing on the selectivity and yield of laser excitations. Following Gorini and Kossakowski[21] we introduce a Hermitian Lindblad-type operator to represent phase relaxation, due to a Gaussian process. We adopt the double commutator form $\mathcal{L}_D\hat{\rho}=-\gamma^*[\hat{H}_0,[\hat{H}_0,\hat{\rho}]]$, where γ^* is a measure for the dephasing rate.[23] The matrix elements are here again very simple in the basis of CIS(D) eigenvectors. With this choice, Eq. (9) remains unchanged while in Eq. (10) the dephasing rate has to be extended by a pure dephasing term, i.e.,

$$\gamma_{mn}\to\gamma_{mn}+\gamma^*\omega_{mn}^2. \tag{12}$$

In lack of a generic model available for the dephasing rate we choose to set $\gamma^*=\tau_{\mathrm{rad}}^{-1}\omega_{20}^{-2}$, where τ_{rad} is the radiative lifetime of state $|2\rangle$, to simulate the regime where dephasing is of comparable magnitude as energy relaxation. Computer experiments were also performed for $\gamma^*=10\tau_{\mathrm{rad}}^{-1}\omega_{20}^{-2}$, $\gamma^*=100\tau_{\mathrm{rad}}^{-1}\omega_{02}^{-2}$, and $\gamma^*=1000\tau_{\mathrm{rad}}^{-1}\omega_{02}^{-2}$ to explore the regimes where dephasing slightly and strongly dominates the radiative lifetime. The pure dephasing times T_2^* between states $|0\rangle$ and $|2\rangle$ thus range from 43 ns to 43 ps in these models.

D. Propagation of the density operator

We transform all operators to the interaction picture by making the substitution $\hat{\rho}(t)=e^{i\hat{H}_0t}\hat{\rho}^I(t)e^{-i\hat{H}_0t}$. We thus obtain

$$\frac{\partial\hat{\rho}^I(t)}{\partial t}=iE_x(t)[e^{-i\hat{H}_0t}\hat{\mu}_xe^{i\hat{H}_0t},\hat{\rho}^I(t)]+e^{-i\hat{H}_0t}\mathcal{L}_De^{i\hat{H}_0t}\hat{\rho}^I(t). \tag{13}$$

In the CIS(D) eigenstate basis the equations of motion then are

$$\frac{d\rho_{mn}^I}{dt}=iE_x(t)\sum_{j=1}^{L}(e^{-i\omega_{mj}t}\mu_{mj}\rho_{jn}^I-e^{-i\omega_{jn}t}\rho_{mj}^I\mu_{jn})+e^{-i\omega_{mn}t}\langle m|\mathcal{L}_D\hat{\rho}|n\rangle. \tag{14}$$

According to the dissipation model described above, matrix elements of the dissipative part of the Liouvillian are, for $m=n$ given as $\langle n|\mathcal{L}_D\hat{\rho}|n\rangle=\Sigma_{i=1}^{L}(\Gamma_{i\to n}\rho_{ii}-\Gamma_{n\to i}\rho_{nn})$ while $\langle n|\mathcal{L}_D\hat{\rho}|n\rangle=-\gamma_{mn}\rho_{mn}$ for $m\neq n$.

To propagate the density operator in the interaction picture, we propose to directly integrate Eq. (14) using an embedded fifth-order Cash–Karp Runge–Kutta integrator with adaptive step size. For that purpose we have made several modifications to the Numerical Recipes procedure,[31] which already proved to be very efficient.[32]

For longer time propagation, e.g., in the nanosecond regime, we advocate using the rotating wave approximation. Although straightforward for a two-level system, the idea is slightly more subtle for a many-level system. Brüggemann *et al.*[33] proposed a Fourier-type expansion for representing the effect of a laser field on an open system in the rotating wave approximation. We prefer the approach developed by Quack[34] for wave-packet propagation, which he calls the quasiresonant approximation (QRA). We will here summarize the most important steps of the method, as applied to the density matrix formalism. The dissipative term will be neglected for presentation, as it is not affected by the QRA treatment. The equations obtained are reminiscent of the work by Domcke and co-workers.[35,36]

We know that, for a single pulse with constant carrier frequency ω, the field is given by $E_x(t)=[S(t)/2](e^{i\omega t}+e^{-i\omega t})$, where $S(t)$ is the shape function of the pulse (sequence). Substituting in Eq. (13) and representing all operators in the basis of CIS(D) eigenstates we have

$$\frac{d\rho_{mn}^I}{dt}=-\frac{S(t)}{2i}\sum_{j=1}^{L}\{(e^{-i(\omega_{mj}-\omega)t}+e^{-i(\omega_{mj}+\omega)t})\mu_{mj}\rho_{jn}^I-(e^{-i(\omega_{jn}-\omega)t}+e^{-i(\omega_{jn}+\omega)t})\rho_{mj}^I\mu_{jn}\}. \tag{15}$$

We then define the transition frequency as a function of the carrier frequency $\omega_{jn}=\alpha_{jn}\omega+\chi_{jn}$, where α_{jn} is an integer chosen so that $\chi_{jn}\in[-\omega/2,\omega/2]$. We substitute in Eq. (15) to obtain the general and exact equation

$$\frac{d\rho_{mn}^I}{dt}=-\frac{S(t)}{2i}\sum_{j=1}^{L}\{(e^{-i(\alpha_{mj}-1)\omega t}+e^{-i(\alpha_{mj}+1)\omega t})\mu_{mj}e^{-i\chi_{mj}t}\rho_{jn}^I-(e^{-i(\alpha_{jn}-1)\omega t}+e^{-i(\alpha_{jn}+1)\omega t})e^{-i\chi_{jn}t}\rho_{mj}^I\mu_{jn}\}. \tag{16}$$

To remove the high frequency components we neglect all terms for which $\alpha_{j_1j_2}\pm1=0$. The equations of motion thus simplify to

$$\frac{d\rho_{mn}^I}{dt}=-\frac{S(t)}{2i}\sum_{j=1,|\alpha_{mj}|=1}^{L}e^{-i\chi_{mj}t}\mu_{mj}\rho_{jn}^I+\frac{S(t)}{2i}\sum_{j=1,|\alpha_{jn}|=1}^{L}e^{-i\chi_{jn}t}\rho_{mj}^I\mu_{jn}. \tag{17}$$

We checked the quality of the QRA for short time propagation, which proved to be very good especially in the weak-field limit. Since only the smooth shape function $S(t)$ appears, long-time steps can be used. Given the density matrix elements in the interaction representation, we can calculate state populations in the Schrödinger picture as

$$\rho_{nn}^I(t)=\rho_{nn}. \tag{18}$$

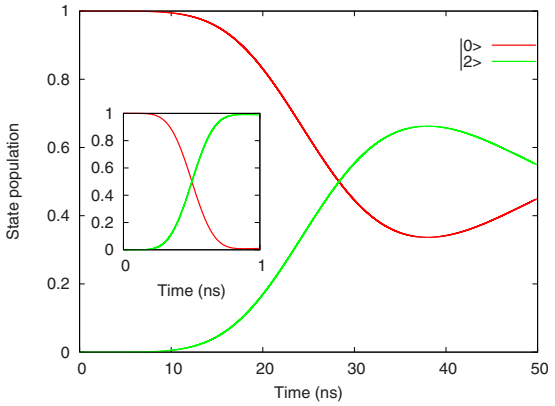

FIG. 2. (Color online) Selective excitation of the charge transfer state, $|2\rangle$, using a 50 ns π-pulse. Spontaneous emission due to coupling to the vacuum has been taken into account. The inset shows the population evolution for 1 ns π-pulse.

III. LASER-PULSE DRIVEN DISSIPATIVE SUBSYSTEM DYNAMICS

A. Selective excitation and switching of a charge transfer state

We first tried to excite selectively the charge transfer state, $|2\rangle$, using a single π-pulse as described in Eq. (4). The "ordinary" spontaneous emission scenario with lifetimes in the regime of tens of nanoseconds and no pure dephasing included was adopted. The pulse length was varied from 100 ps to 100 ns, from significantly shorter to longer than the radiative lifetime of the target state. The average time step for the propagations was found to be on the order of 1 fs for all excitations performed. The maximal field intensity for a π-pulse is given by $I=\frac{1}{2}\epsilon_0 c E_0^2$. For a 1 ns pulse with frequency tuned at the $0\rightarrow 2$ transition we find $I=8456\ \mathrm{W/cm^2}$, which is well within the pertubative regime. While correct for short time evolution the perturbative treatment is expected to yield qualitatively incorrect results when reaching population saturation. The current approach does not suffer from this drawback.

The evolution of the population of state $|2\rangle$ and the ground state is shown in Fig. 2 for 1 and 50 ns pulses. For long-time propagations it would be very costly to use the full basis of 186 CIS(D) eigenstates to perform the dynamics. We therefore choose to truncate the basis at the 20th excited state, where there is a larger gap in the energy distribution. We checked convergence of the selected subset of eigenstates by performing dynamics with the full basis, as well as with another subset of 41 eigenstates, for a 1 ns π-pulse excitation. The results proved to be numerically equivalent.

It can clearly be seen from Fig. 2 that it is not possible to reach complete population transfer with the 50 ns pulse, whereas the effect of dissipation is negligible for the 1 ns excitation dynamics (see inset). All states not represented in the figure are not significantly populated and the actual dynamics could be reduced to a two-state system in both cases. This can be explained by the very long duration of the pulse and its very low intensity. Only for significantly shorter, more intense pulses higher-excited states are populated and need to be included in the propagation. The energy of the laser is thus well defined and no dynamic broadening nor multiphoton excitation occur. The selectivity of the charge transfer is therefore perfect although the yield varies with the pulse duration, as one would expect.

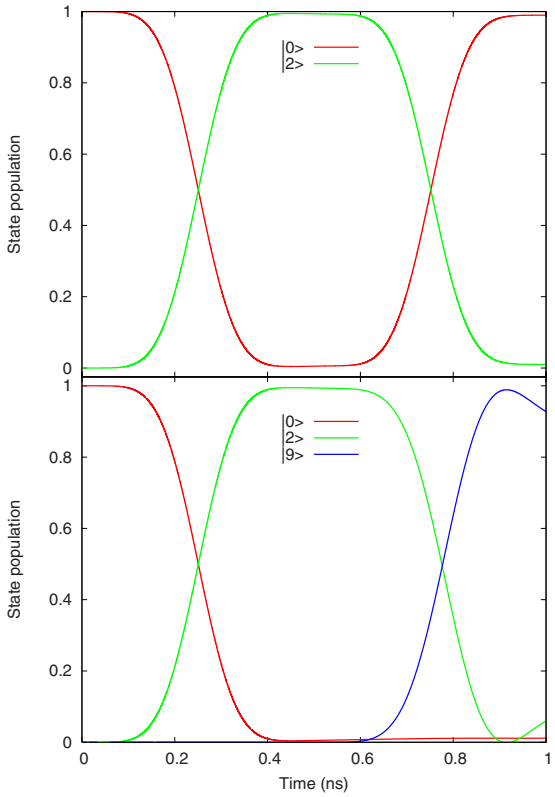

FIG. 3. (Color online) Control of the dipole switching dynamics in presence of radiative decay using two consecutive π-pulses. Top panel: population evolution for the sequence $|0\rangle\rightarrow|2\rangle\rightarrow|0\rangle$. Bottom panel: population evolution for the sequence $|0\rangle\rightarrow|2\rangle\rightarrow|9\rangle$.

Figure 3 shows the population evolution for simple dipole switching control experiments. A first carrier frequency is used for exciting the $|2\rangle$ state from $|0\rangle$, and a second one is used for the later de-excitation or excitation of the $|9\rangle$ state. We chose to use two 500 ps π-pulses using the truncated basis described above.

Even despite the 500 ps pulses are shorter than the lifetimes, it is already possible to see the effects of dissipation. At the top panel it appears that energy relaxation has very little influence, as the first π-pulse almost completely transfers population to state $|2\rangle$. The subsequent de-excitation is about as efficient and only about 1% population remains in the excited state. On the bottom panel we can see that population transfer is also very efficient for the $|2\rangle\rightarrow|9\rangle$ excitation, as negligible population remains in the intermediate state. An interesting feature is that about 1% population is found in the ground state after the second pulse. This is purely due to dissipation since no significant dynamic broadening occurs for such long and weak electric fields. This shows also that the system has a memory of the previous excitations. To confirm this hypothesis we have used a series of 20 nonoverlapping 500 ps π-pulses with frequency $\omega=\omega_{20}$. It can be seen from Fig. 4 that the transfer yield decreases as the number of pulse increases even though each single pulse is significantly shorter than the state lifetime.

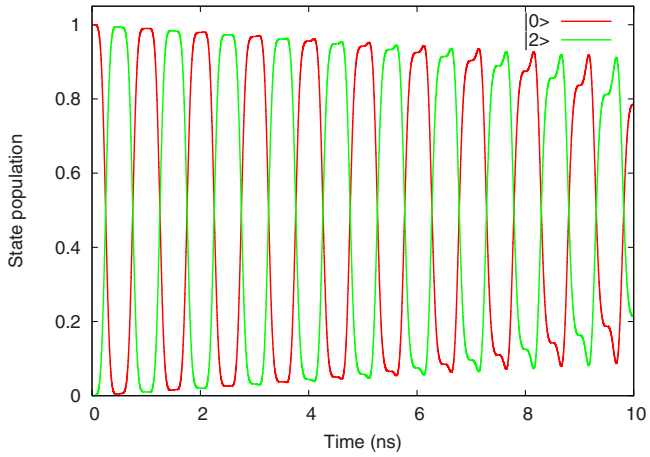

FIG. 4. (Color online) Control of the dipole switching dynamics in the presence of radiative decay using a train of consecutive π-pulses.

The dissipation thus appears to have a cumulative effect on the excitation dynamics, primarily due to the decay of the excited state population between the pulses.

B. Surface enhanced relaxation approach

Focusing on the ultrashort time dynamics we can study the effect of the SERA model for energy relaxation on selective excitation of states $|2\rangle$ and $|9\rangle$. The lifetimes of the states of interest are 430 fs and 3.6 ps, respectively. The full basis of 186 CIS(D) approximate eigenstates was used for the propagations. For pulses in the femtosecond regime, it was found that the average time step for the propagations is on the order of 0.01 fs, with slightly shorter time steps for higher field fluences. We have optimized the length of a π-pulse to achieve the maximal population of state $|2\rangle$. Figure 5 shows the population dynamics for the optimal pulse length of 75 fs and maximal field intensity $I=1.50\times10^{12}$ W/cm^2, which lies clearly in the strong field regime.

We see that even on this very short time scale, the effects of energy relaxation are well present. For longer π-pulses dissipation starts to dominate and less population transfer occurs. It is interesting to note that the excitation is very selective, as only state $|5\rangle$ is minimally populated at about 30 fs and all the population remains in either the ground state or the target state. On the other hand, for shorter π-pulses, dynamic broadening and, more importantly, multiphoton excitation becomes the dominant factor and the transfer yield is also reduced (see inset). The maximal field intensity of the latter 5 fs π-pulse is very high ($I=3.37\times10^{14}$ W/cm^2). As a consequence, state selectivity is completely lost and a broad range of electronic levels is excited. Furthermore, for such large intensities, ionization becomes a dominant process and should therefore be taken into account. The scaling of the SERA model being largely arbitrary, these results represent only typical excitation dynamics behavior for short dissipative lifetimes.

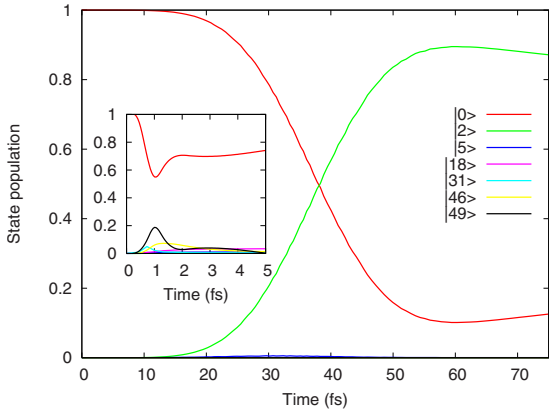

FIG. 5. (Color online) Selective excitation of the charge transfer state, $|2\rangle$, using a 75 fs π-pulse. The SERA model for dissipation has been considered. The inset shows the population evolution for a 5 fs π-pulse.

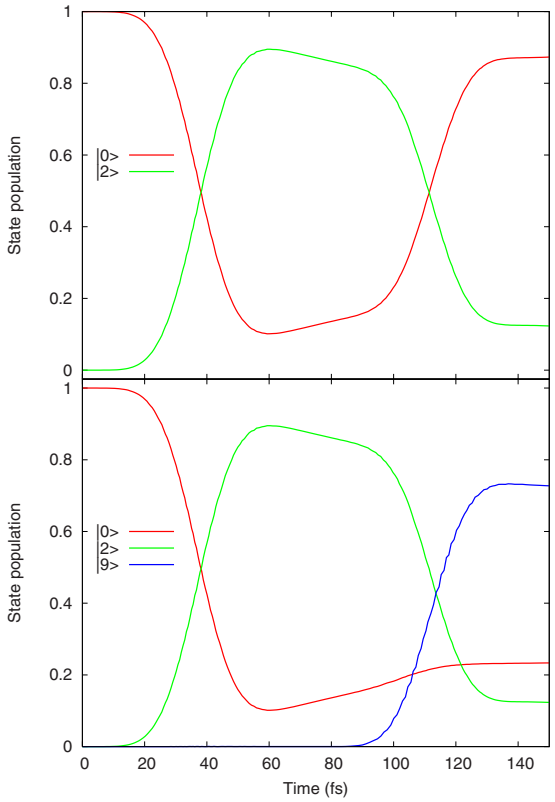

FIG. 6. (Color online) Control of the dipole switching dynamics with a sequence of consecutive π-pulses using the SERA model for dissipation. Top panel: population evolution for the sequence $|0\rangle\rightarrow|2\rangle\rightarrow|0\rangle$. Bottom panel: population evolution for the sequence $|0\rangle\rightarrow|2\rangle\rightarrow|9\rangle$.

We studied again the dipole switching dynamics for the SERA model. We used the optimized pulse length to excite the charge transfer state as a first step for both $|0\rangle\rightarrow|2\rangle\rightarrow|0\rangle$ and $|0\rangle\rightarrow|2\rangle\rightarrow|9\rangle$ excitation pathways. The same pulse was used to depopulate state $|2\rangle$ in the first case. We also optimized the pulse length for the second excitation in the second case. The population evolution of the two excitation pathways can be seen from Fig. 6.

From the top panel it appears clearly that dissipation reduces the yield of dipole switching without affecting selectivity. The population in the ground state at the end of the second pulse is about 90%, the same as that of the charge transfer state at the end of the first pulse. As for the second pathway the optimal pulse achieves only partial population transfer to the state of interest. In the meantime the ground

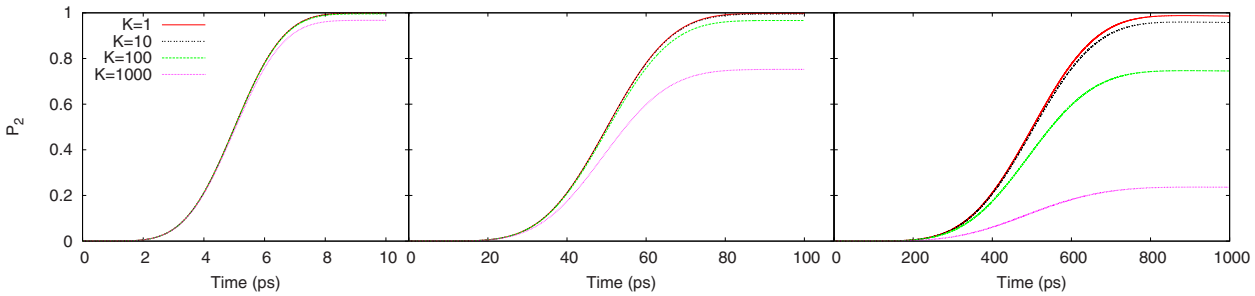

FIG. 7. (Color online) Effect of pure dephasing on selective excitation of the charge transfer state, $|2\rangle$. From left to right: $|2\rangle$ state population evolution using 10 ps, 100 ps, and 1 ns π-pulses, respectively. The pure dephasing rates between $|0\rangle$ and $|2\rangle$ are given as $K\tau_{\mathrm{rad}}$, where the radiative lifetime of state $|2\rangle$ is $\tau_{\mathrm{rad}}=43$ ns.

state gets also populated and part of the population remains in state $|2\rangle$. The selectivity of the excitation is thus slightly reduced in this particular case.

C. Pure dephasing

To evaluate the effect of pure dephasing, four different dephasing rates were introduced for the case where it is of comparable magnitude to the energy relaxation mechanism, and also for cases where it dominates slightly or strongly ($\gamma^{*}=K\tau_{\mathrm{rad}}^{-1}\omega_{02}^{-2}$ with $K=1,\ 10,\ 100,\ 1000$). The population evolution of state $|2\rangle$ upon excitation with π-pulses of durations 10 ps, 100 ps, and 1 ns can be seen in Fig. 7. For 1 ps pulses and shorter, pure dephasing plays no significant role within these models.

In all cases perfect state selectivity was achieved, i.e., only state $|2\rangle$ is excited. However, the excitation probability is strongly dependent on the dephasing rates. Using the 10 ps pulse (left panel) the dynamics of the system is not affected by pure dephasing for moderate to medium dephasing rates, i.e., $K=1,\ 10,\ 100$. On this time scale the population transfer is complete. The situation is slightly different for very fast dephasing, where only about 95% of the population is transferred. Increasing the pulse duration (see middle panel) we see that this effect becomes more dramatic as less than 80% population transfer is achieved for the fastest dephasing. The off-diagonal elements of the subsystem density matrix vanish quickly to damp the excitation efficiency. For the longest dephasing times ($K=1,\ 10$) the population inversion is still almost complete. For longer pulses both pure dephasing and energy relaxation can play a significant role. At the right panel of Fig. 7 we can see the damping effect of pure dephasing on population transfer as, even for the smallest dephasing rate, the population transfer is not complete (see the inset of Fig. 2 for a comparison). For a moderate rate the population transfer is flattened and reaches only slightly more than 20% in the very fast dephasing case. It can be said that, although the model presented here is limited, the effect of pure dephasing can be systematically studied within the reduced density matrix framework.

IV. CONCLUSION

In conclusion, we have proposed an extension of the TD-CI method to perform selective electronic excitations of lithium cyanide. The reduced density matrix formalism was used to include effects of energy and phase dissipation on the electron dynamics. Lindblad-type operators were introduced to study the energy relaxation mechanism as well as pure dephasing.

The radiative lifetimes corresponding to spontaneous emission were evaluated using Einstein coefficients, which have a cubic energy dependence. The resulting lifetimes were found in the nanosecond regime and a scaled variant was proposed to simulate an electron-rich medium, such as a metal surface, favoring energy dissipation. These models go beyond the fixed rate approach proposed by Di Ventra and D'Agosta.[6] In addition, a Kossakowski-type model for Gaussian pure dephasing gave rise to dephasing times depending quadratically on the energy gap. The QRA was extended to the reduced density matrix to perform long-time propagation, coupled with an adaptive step-size Cash–Karp Runge–Kutta integrator in the interaction picture.

The results showed that, in most cases, energy relaxation does not represent a major problem to achieve state selectivity of the charge transfer and dipole switching excitations. In particular "normal" spontaneous emission, which proceeds on a nanosecond time scale, does not alter the dissipation-free dynamics at all if not too long pulses are used. In general, however, the excitation yield can be diminished by both energy relaxation and pure dephasing on the time scale relevant for each model. It was also seen that, for very short pulses even when dissipation becomes negligible, energy broadening and multiphoton excitation dominates the population dynamics. State selectivity, as well as the transfer yield, are completely lost in this case. These effects are further enhanced by dissipation.

The approach presented here is a very natural extension of the TD-CI formalism for wavepacket dynamics and its applicability is only limited by the quality of the CI calculations. The latter is certainly restricted on the CIS and even CIS(D) levels of theory, however, it can at least in principle be systematically improved toward the full-CI limit.[37] The biggest approximation made in this exploratory study is the fixed-nuclei approximation, which certainly would not hold in practice for excitation of CT states of free LiCN with ns laser pulses. Ionization processes, which will occur when excited states above the vacuum level are temporarily populated, have also been neglected so far. A straightforward way to circumvent this problem is by replacing the CI energies E_i by energies $E_i-i(\Gamma_i/2)$ in the propagation, where Γ_i is the

ionization rate of state $|i\rangle$. As a further refinement, optimal control schemes[38,39] would also be useful for improving selectivity and efficiency of controlled dissipative electron dynamics.

In general, we expect the new scheme to be of great use for all electron dynamics applications where good energies and dipole moments can be obtained and where dissipation plays a role. Apart from quantum transport through junctions, the photophysics of quantum dots or of adsorbates at surfaces[40] represent good examples of such systems.

ACKNOWLEDGMENTS

This work was supported by the Fonds Québécois de la Recherche sur la Nature et les Technologies (FQRNT) and the Sonderforschungbereich 658 of the Deutsche Forschungsgemeinschaft, *Elementary processes in molecular switches at surfaces* (subproject C2).

[1] A. Szabo and N. S. Ostlund, *Modern Quantum Chemistry* (Dover, Mineola, 1996).
[2] P. Hohenberg and W. Kohn, Phys. Rev. **136**, B864 (1964).
[3] W. Kohn and L. Sham, Phys. Rev. **140**, A1133 (1965).
[4] E. Runge and E. K. U. Gross, Phys. Rev. Lett. **52**, 997 (1984).
[5] S. K. Ghosh and A. K. Dhara, Phys. Rev. A **38**, 1149 (1988).
[6] M. Di Ventra and R. D'Agosta, Phys. Rev. Lett. **98**, 226403 (2007).
[7] M. Di Ventra and R. D'Agosta, e-print arXiv:cond-mat/08053734.
[8] K. C. Kulander, Phys. Rev. A **36**, 2726 (1987).
[9] T. Klamroth, Phys. Rev. B **68**, 245421 (2003).
[10] M. Nest, T. Klamroth, and P. Saalfrank, J. Chem. Phys. **122**, 124102 (2005).
[11] J. Zanghellini, M. Kitzler, C. Fabian, T. Brabec, and A. Scrinzi, Laser Phys. **13**, 1064 (2003).
[12] T. Kato and H. Kono, Chem. Phys. Lett. **392**, 533 (2004).
[13] C. Huber and T. Klamroth, Appl. Phys. A: Mater. Sci. Process. **81**, 91 (2004).
[14] P. Saalfrank, T. Klamroth, C. Huber, and P. Krause, Isr. J. Chem. **45**, 205 (2005).
[15] P. Krause, T. Klamroth, and P. Saalfrank, J. Chem. Phys. **123**, 074105 (2005).
[16] T. Klamroth, J. Chem. Phys. **124**, 144310 (2006).
[17] S. Klinkusch, T. Klamroth, and P. Saalfrank (unpublished).
[18] A. Thon, M. Merschdorf, W. Pfeiffer, T. Klamroth, P. Saalfrank, and D. Diesing, Appl. Phys. A: Mater. Sci. Process. **78**, 189 (2004).
[19] H. Schlegel, S. Smith, and X. Li, J. Phys. Chem. **126**, 244110 (2007).
[20] V. Gorini, A. Kossakowski, and E. C. G. Sudarshan, J. Math. Phys. **17**, 821 (1976).
[21] V. Gorini and A. Kossakowski, J. Math. Phys. **17**, 1298 (1976).
[22] G. Lindblad, Commun. Math. Phys. **48**, 119 (1976).
[23] R. Kosloff, M. Ratner, and W. B. Davis, J. Chem. Phys. **106**, 7036 (1997).
[24] D. M. Lockwood, M. Ratner, and R. Kosloff, Chem. Phys. **268**, 55 (2001).
[25] E. A. Weiss, G. Katz, R. H. Goldsmith, M. R. Wasielewski, M. Ratner, R. Kosloff, and A. Nitzan, J. Chem. Phys. **124**, 074501 (2006).
[26] M. Head-Gordon, R. J. Rico, M. Oumi, and T. J. Lee, Chem. Phys. Lett. **219**, 21 (1994).
[27] M. W. Schmidt, K. K. Baldridge, J. A. Boatz, S. T. Elbert, M. S. Gordon, J. H. Jensen, S. Koseki, N. Matsunaga, K. A. Nguyen, S. Su, T. L. Windus, M. Dupuis, and J. A. Montgomery, Jr., J. Comput. Chem. **14**, 1347 (1993).
[28] Upon energy sorting, we find one more nondegenerate state at $0.263698E_h$ than in Ref. 15. The total number of states and their energies being the same, we attribute this difference to wrong energy ordering. The conclusions presented by the authors remain valid as they merely rely on energy ordering for state labeling. The states $|7\rangle$ and $|8\rangle$ in Ref. 15 thus corresponds to states $|8\rangle$ and $|9\rangle$ used here.
[29] K. Blum, *Density Matrix Theory and Applications* (Plenum, New York, 1996).
[30] P. Saalfrank, Chem. Rev. (Washington, D.C.) **106**, 4116 (2006).
[31] W. H. Press, S. A. S. A. Teukolsky, W. T. Vetterling, and B. P. Flannery, *Numerical Recipes in FORTRAN 77 The Art of Scientific Programming* (Cambridge University Press, Cambridge, 1986).
[32] J. C. Tremblay and T. Carrington, Jr., J. Chem. Phys. **121**, 11535 (2004).
[33] B. Brüggemann, T. Pullerits, and V. May, J. Photochem. Photobiol., A **190**, 372 (2007).
[34] M. Quack, J. Chem. Phys. **69**, 1282 (1978).
[35] L. Seidner, G. Stock, and W. Domcke, J. Chem. Phys. **103**, 3998 (1995).
[36] B. Wolfseder, L. Seidner, G. Stock, and W. Domcke, Chem. Phys. **217**, 275 (1997).
[37] P. Krause, T. Klamroth, and P. Saalfrank, J. Chem. Phys. **127**, 034107 (2007).
[38] Y. Ohtsuki, K. Nakagami, W. Zhu, and H. Rabitz, Chem. Phys. **287**, 197 (2003).
[39] S. Beyvers, Y. Ohtsuki, and P. Saalfrank, J. Chem. Phys. **124**, 234706 (2006).
[40] H. Petek, M. Weida, H. Nagano, and S. Ogawa, Science **288**, 1402 (2000).